Supplementary material and poster for:

A NEW MAGNITUTE-BASED APPROACH TO DETECT YEAR-ROUND WARM SPELLS AND THEIR RECENT INTENSIFICATION

THE CYPRUS INSTITUTE
RESEARCH·TECHNOLOGY·INNOVATION

HELLENIC REPUBLIC
National and Kapodistrian University of Athens
EST. 1837

Presenter: Aristotelis Liakakos
Evangelos Tyrlis, Panos Hadjinicolaou, George Zittis
a.liakakos@cyi.ac.cy

EGU26
GENERAL ASSEMBLY

Poster presentation
Natural Hazards – Session NH1.9
(Extreme heat: characterization, drivers, prediction and impacts in a warming climate)

Funded by the European Union

!PREVENT

OptimESM
Optimal high resolution Earth System Models for exploring future climate change

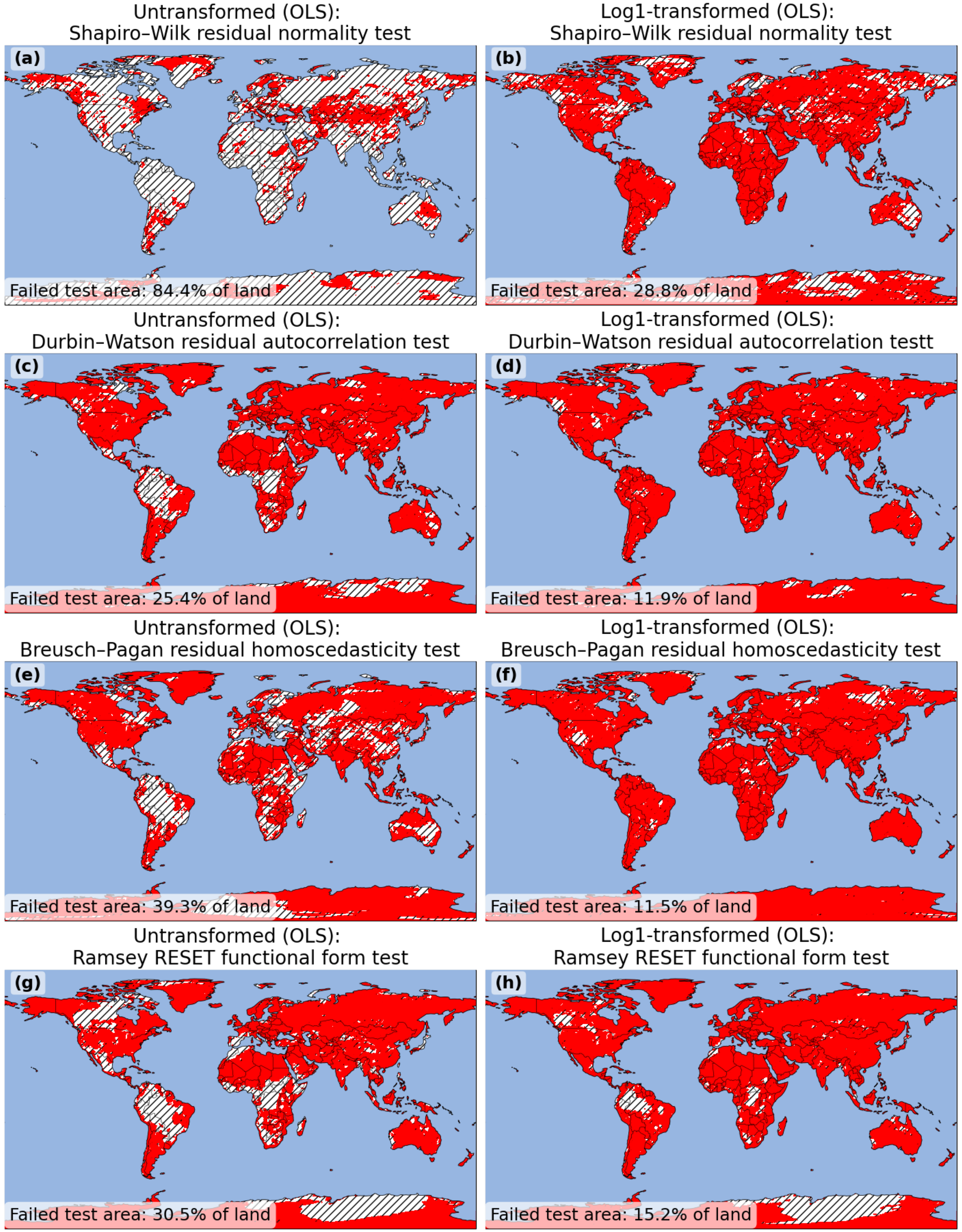

Supplementary Figure 1. Global pass/fail maps of ordinary least squares (OLS) regression diagnostic tests applied at each land grid point for yearly summed WSMId over the period 1980–2024, complimenting Figure 4. The left column shows regressions using untransformed WSMId, while the right column shows regressions using logarithmically-transformed WSMId. Panels (a–b) show the Shapiro–Wilk residual normality test, (c–d) the Durbin–Watson residual autocorrelation test, (e–f) the Breusch–Pagan residual homoscedasticity test, and (g–h) the Ramsey RESET functional form test (power = 2). Red shading indicates grid points where the respective diagnostic is passed, while hatched regions indicate failure of the test. Passing criteria are defined as $p > 0.05$ for p-value–based tests and Durbin–Watson statistics within the range 1.5–2.5. Percentages denote the fraction of total land area failing each diagnostic, computed using area-weighted land grid-cell areas.

- Simple linear regression (SLR) relies on **key assumptions**, including residual normality, independence, homoscedasticity, and linearity.
- These assumptions are evaluated using **standard diagnostic tests**.
- Panels (a, c, e, g) show diagnostics for SLR applied to non-transformed yearly summed WSMId, while panels (b, d, f, h) show the same diagnostics applied after logarithmic transformation.
- The log-transformed **SLR exhibits substantially improved diagnostic performance, indicating a better adherence to model assumptions**.
- This supports the use of an exponential model for trend analysis, **consistent with an accelerating increase in warm spell load!**

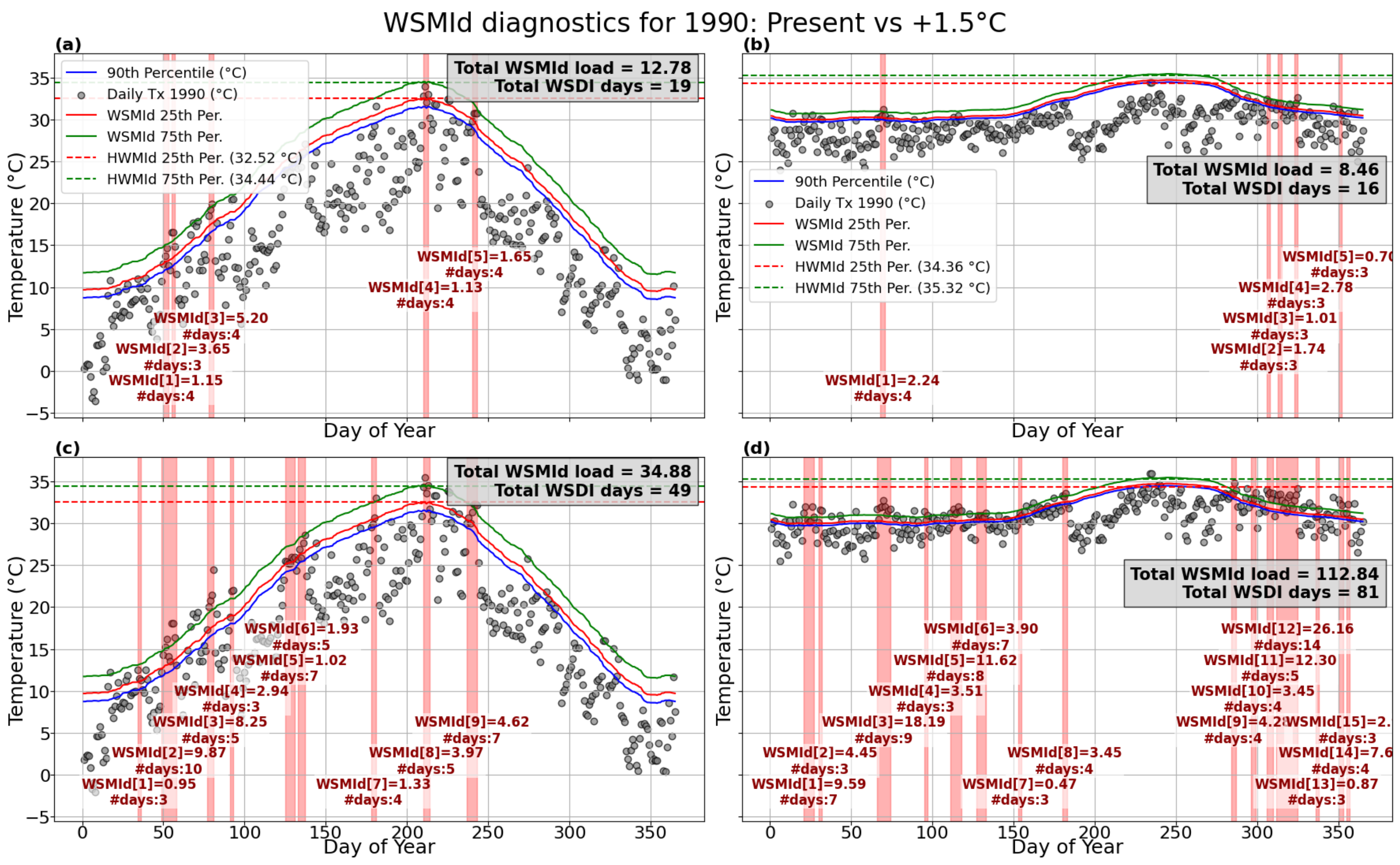

Supplementary Figure 2. Grid-point examples of warm spell detection and magnitude diagnostics, shown in a format analogous to Fig. 1 applied to ERA5 grid cells and extended to a +1.5°C warming experiment. Panels (a) and (b) show 1990 conditions for Central European and Central-West South American grid-point, respectively, while panels (c) and (d) show the corresponding +1.5°C simulations.

- Figure 4 shows the largest ratios of change concentrated in equatorial regions over Africa and South America.
- In these regions, the annual temperature cycle and interannual variability are relatively small compared to higher latitudes. As a result, even modest background warming leads to a substantial increase in exceedances of fixed percentile thresholds.
- This amplifies the response of percentile-based indices (e.g., WSDI, WSMId), producing disproportionately large increases in warm spell metrics.
- This behaviour reflects a transition toward a quasi-persistent exceedance regime of the 90th percentile, driven by the combination of low variability and systematic warming.

A NEW MAGNITUTE-BASED APPROACH TO DETECT YEAR-ROUND WARM SPELLS AND THEIR RECENT INTENSIFICATION

The Cyprus Institute — Research · Technology · Innovation

Hellenic Republic — National and Kapodistrian University of Athens — Est. 1837

Aristotelis Liakakos[1,2], Evangelos Tyrlis[2], Panos Hadjinicolaou[1], George Zittis[1]

[1]Climate and Atmosphere Research Center (CARE-C), The Cyprus Institute

[2]National and Kapodistrian University of Athens, Department of Physics

1. Introduction

What is a warm spell?

Prolonged periods of extreme anomalous warmth, or else "warm spells", have increased dramatically in **magnitude, duration, frequency** and **spatial extend,** altering ecosystems, agriculture and imposing health impacts**.**

A. Can we quantify warm spells consistently across the year?

B. How much have warm spells changed since 1980?

C. What about their spatial extent?

2. Data & Methods

A. Can we quantify warm spells consistently across the year?

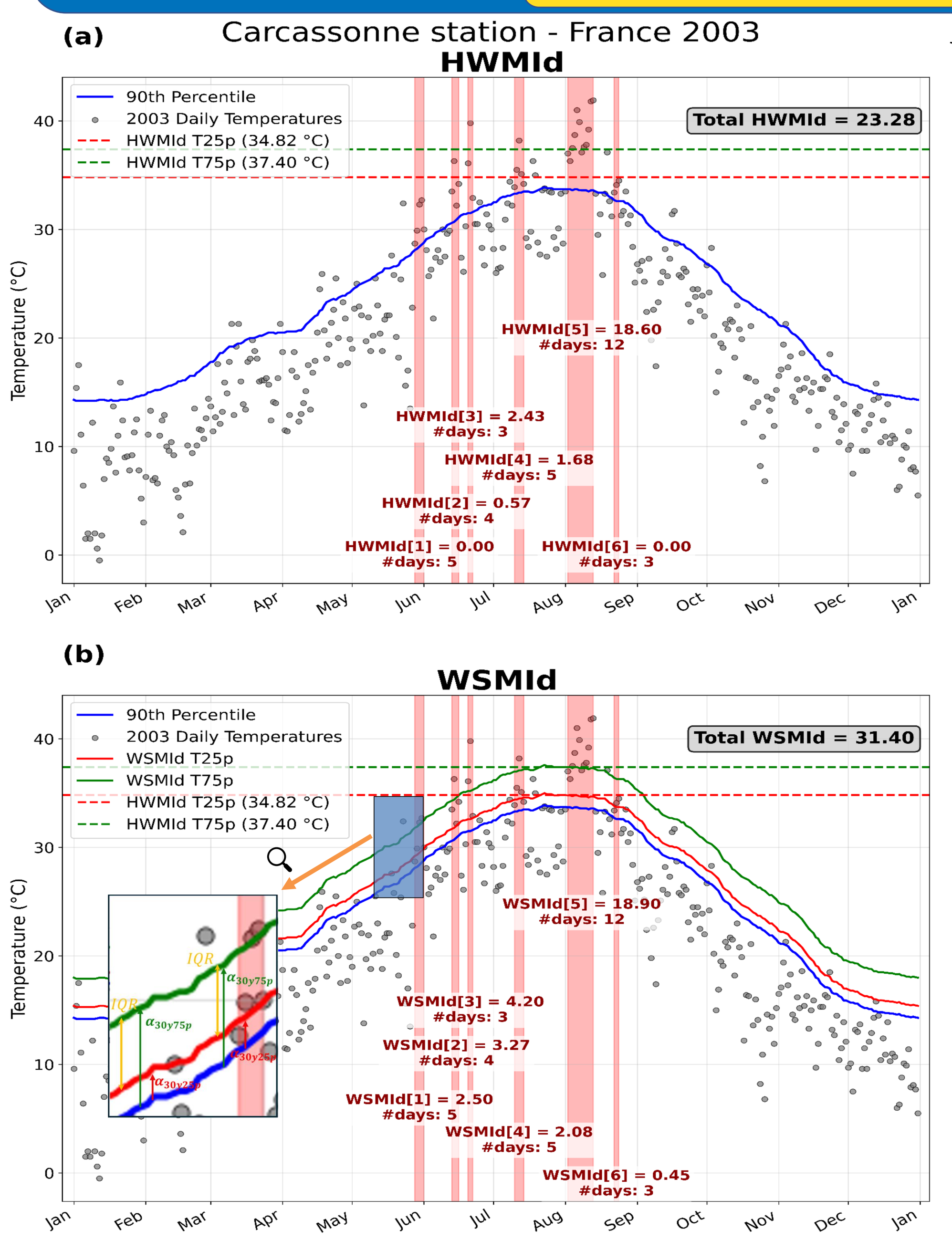

Figure 1 | Daily maximum temperature (T_x) at Carcassonne in 2003, illustrating warm spell detection and magnitude for HWMId (a) and WSMId (b), with the 90th percentile threshold and corresponding reference levels. Warm spells are highlighted, with annotations indicating magnitude and duration.

Warm Spell Magnitude Index daily (WSMId):

➢ Quantifies the magnitude of prolonged anomalous warm events year-round.

➢ Extending the existing heat-wave specialized **Heat Wave Magnitude Index daily (HWMId)**

1. Requirements
Daily T_x (ERA5 | 1980-2024), 30-year reference period (1981-2010)

2. Warm spell detection (T_d)
≥ 3 consecutive days with T_x >90th percentile (31-day moving window.)

3. WSMId modification
Using the 25th and 75th percentiles of warm spell anomalies from the 90th percentile, we calculate: T_{30y25p}, T_{30y75p}

4. Normalization

if $T_d < T_{30y25p}$: $M_d(T_d) = 0$

if $T_d > T_{30y25p}$: $M_d(T_d) = \frac{T_x - T_{30y25p}}{T_{30y75p} - T_{30y25p}}$

5. Summation over:
an event = **Warm spell severity**
a period = **Warm spell load**

3. Results

A. Can we quantify warm spells consistently across the year?

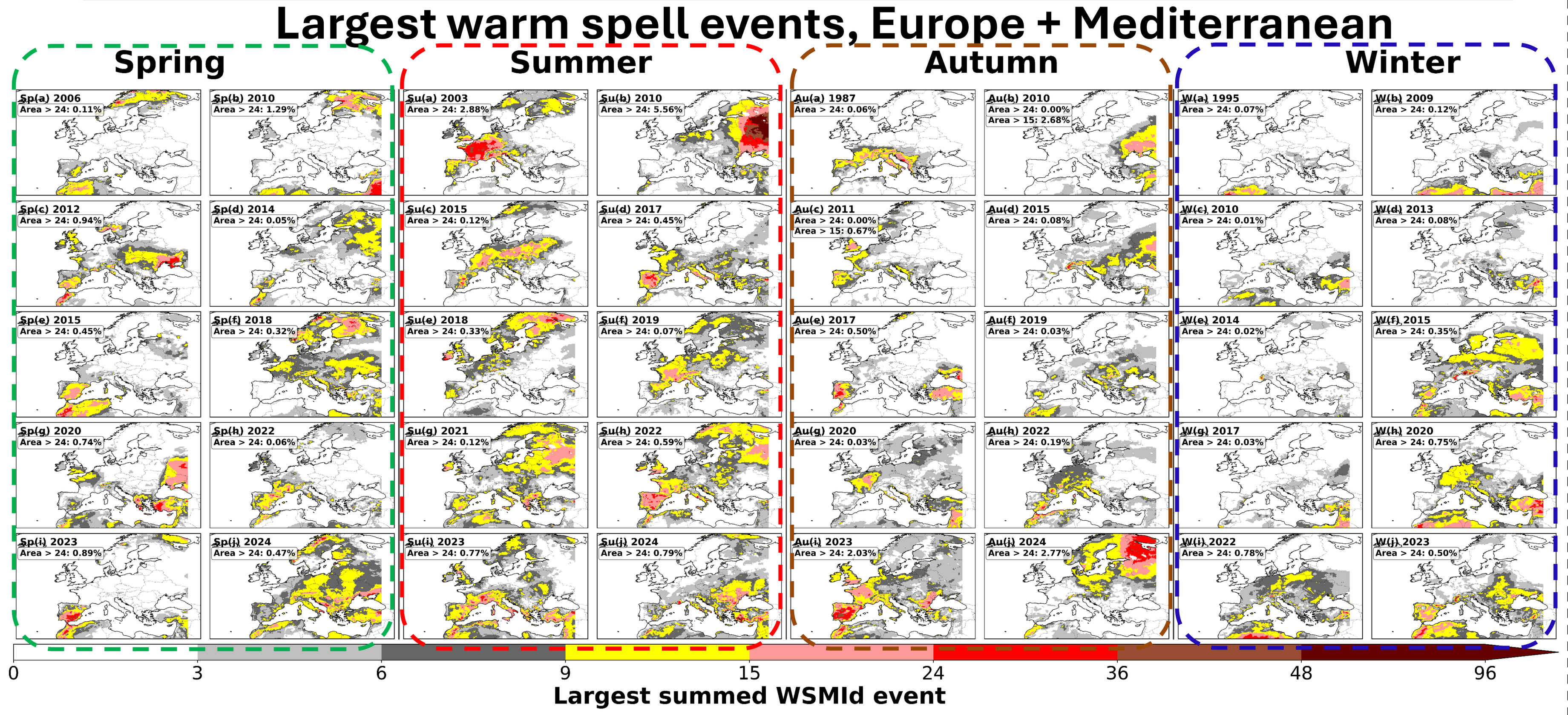

Figure 2 | Spatial distribution of the 10 largest warm spell events over the European–Mediterranean AR6 regions (16, 17, 19) from ERA5, for every season for the period 1980-2024. Events are ranked by the affected area exceeding WSMId > 24 and WSMId > 15 following Russo et al., 2015, with the legend indicating total impacted area.

- WSMId enables **year-round warm spell ranking**.
- Autumn 2023 & 2024 events are **comparable** to 2003 mega heatwave.
- **26/40 largest warm spell** events took place **during the latest decade, 15 of those in the last 5 years!**

B. How much have warm spells changed since 1980?

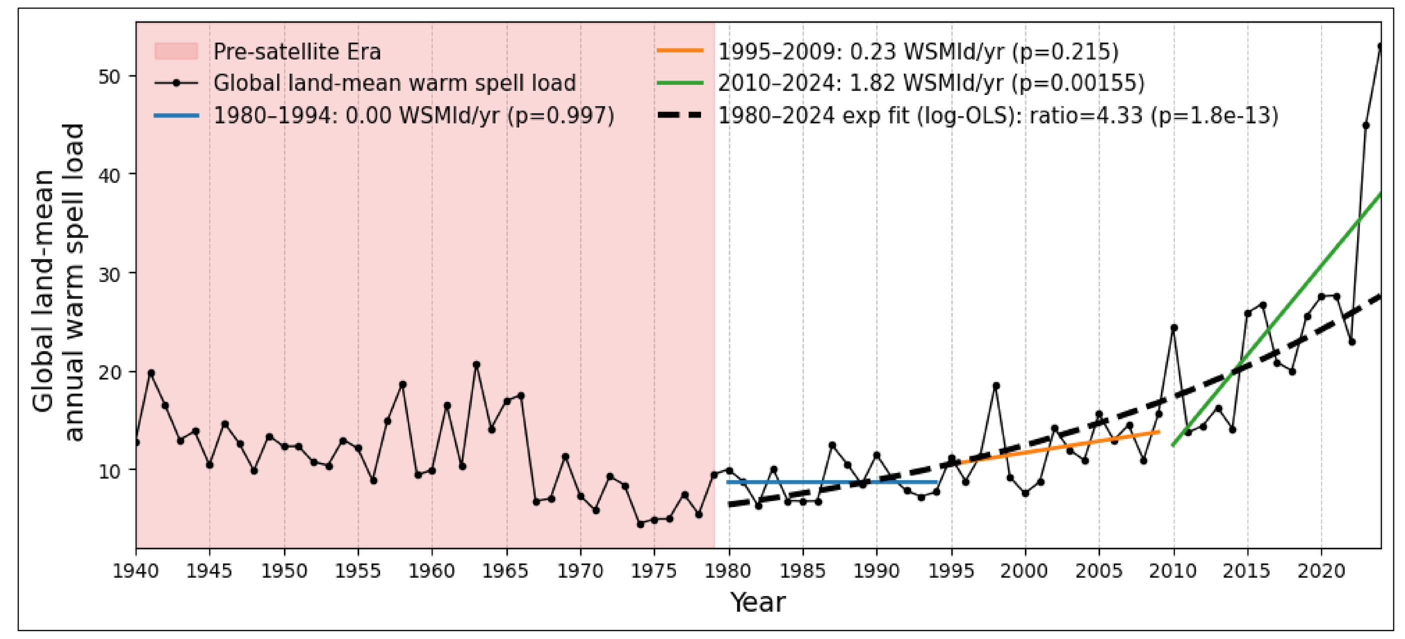

Figure 3 | Global land-mean annual WSMId from ERA5 (1940–2024), with the pre-satellite period (1940–1979) shaded. Piecewise linear trends (1980–1994, 1995–2009, 2010–2024) and an exponential fit (1980–2024). Statistical significance p-values shown follow Student's t-test.

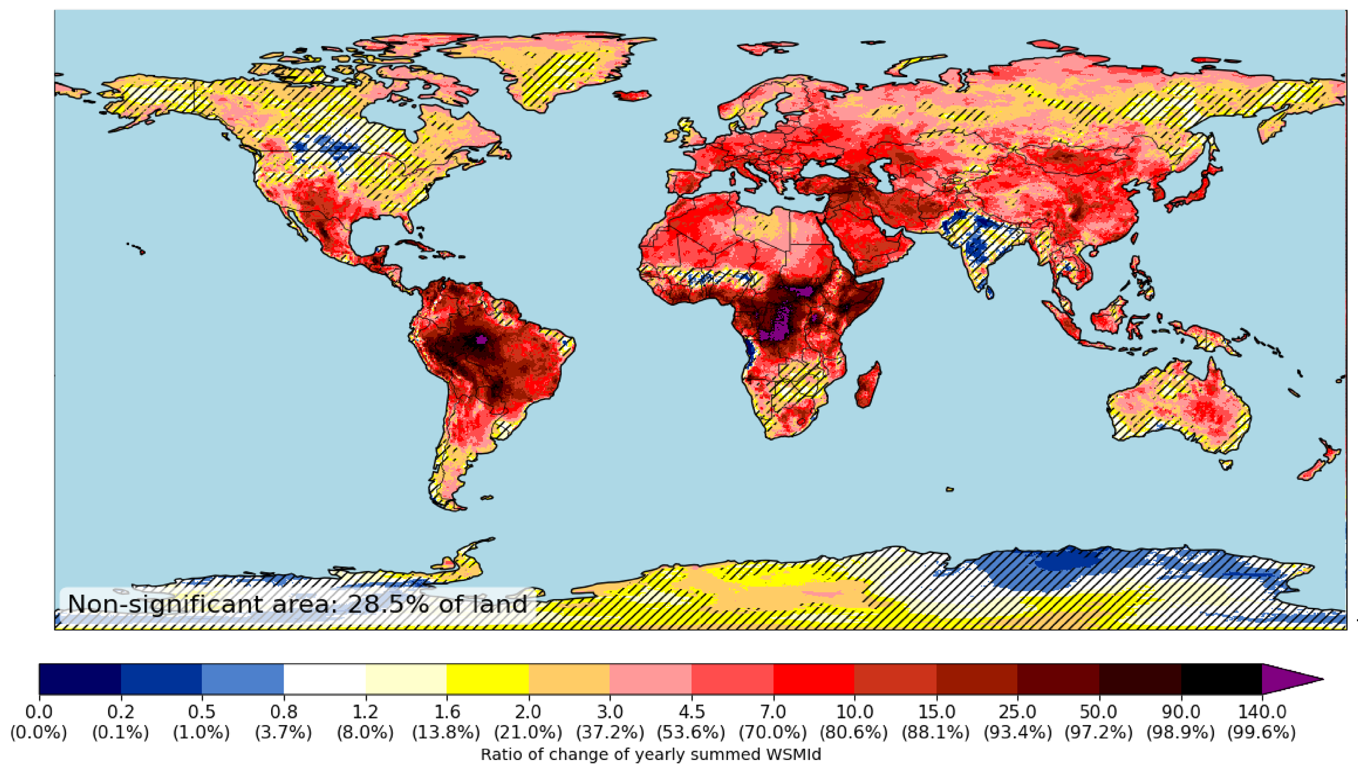

Figure 4 Ratio of change in annual WSMId (warm spell load) over 1980–2024 from ERA5, derived using log-transformed OLS trends. Hatching indicates statistically insignificant areas (p > 0.05, Student's t-test), and parentheses denote cumulative land area fractions.

- Global annual warm spell load **increased by a factor larger than 4 during 1980-2024**!
- An exponential trend analysis fit performed better than the linear one, indicating **the acceleration** of events.
- Globally, the exponential trend fit is **statistically significant over more than 70% of land**, supporting an **accelerating increase**.
- More than **45% of land** have a **ratio of change ≥ 4.5** during 1980-2024!

C. What about their spatial extent?

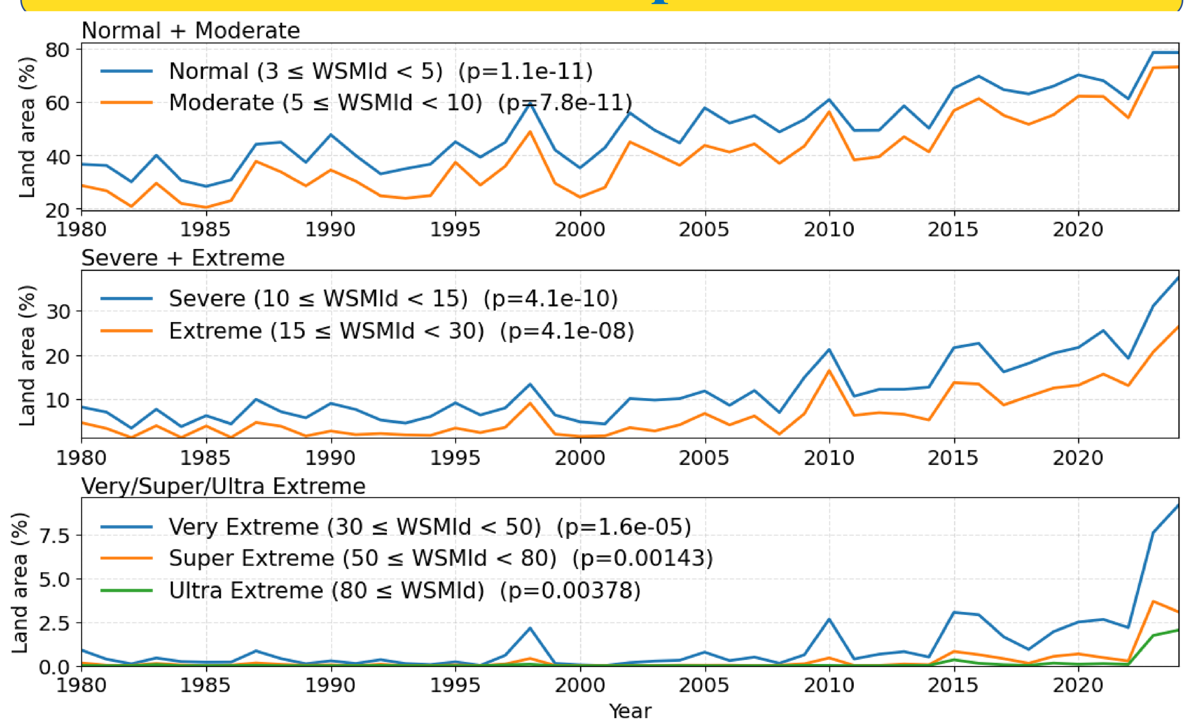

Figure 5 Global land-area percentages of different WSMId event severity classes where at least one warm spell in each class, with p-value following Mann-Kendall test for monotonicity.

- Warm spells are becoming common, **substantially increasing in all severity levels.**
- **Upper extreme classes**, once only reported in climate predictions, **are now here**!

4. Conclusions

➢ **WSMId quantifies warm spell magnitude consistently throughout the year, enabling comparison across seasons.**

➢ **Ranking of the largest seasonal warm spells yielded significant intensification over the past decade.**

➢ **Global annual warm spell load is increasing, at an accelerating rate.**

➢ **Each year, warm spells cover larger areas across every severity class.**

Vote here! ☺

Acknowledgements

This research has been supported by the OptimESM project, which has received funding from the European Union's Horizon Europe Research and Innovation Programme under grant agreement no. 101081193 and the PREVENT project that has received funding from the European Union's Horizon Europe Research and Innovation Programme under Grant Agreement No. 101081276.